Thin Solid Films 536 (2013) 256–260

Contents lists available at SciVerse ScienceDirect

Thin Solid Films

journal homepage: www.elsevier.com/locate/tsf

The effect of 200 MeV Ag ions on the transport property of yttrium barium copper oxide/silver composite thin film

A. Kujur [a], K. Asokan [b], D. Behera [a,*]

[a] Department of Physics, National Institute of Technology, Rourkela-769 008, India
[b] Inter University Accelerator Centre, Aruna Asaf Ali Marg, New Delhi-110 067, India

ARTICLE INFO

Article history:
Received 29 June 2012
Received in revised form 23 March 2013
Accepted 25 March 2013
Available online 6 April 2013

Keywords:
YBCO
Swift heavy ion
Critical current density
Pinning centre
Flux pinning

ABSTRACT

$YBa_2Cu_3O_{7-x}$/Ag (3 at.%) composite thin films are grown by pulsed laser deposition. The films are irradiated with 200 MeV silver ions at room temperature. X-ray diffraction and Raman techniques are used for microstructural disorder analysis. The fall in the intensity of the peaks after irradiation gives a clue of amorphization occurring in the sample. Raman spectra show the loss of apical oxygen O (4) at 500 cm^{-1} and a defect peak appearing at 600 cm^{-1} on irradiation. Magnetization vs. field loop is recorded at 40 K. The synergistic impact of Ag and columnar defects generated by irradiation, deteriorate material property and impedes the flow of supercurrent thereby resulting in decrease of critical current density and flux pinning.

1. Introduction

The high temperature superconductor (HTSC) $YBa_2Cu_3O_{7-x}$ (YBCO) is uniquely characterized by short coherence length (ξ), large planar anisotropy and high transition temperature (T_c). However, the important variable of research interest is the critical current density (J_c). Owing to its exceptionally small ξ, even minor structural imperfections such as grain boundary block the supercurrent in YBCO. Hence research quest is constantly focusing on the increase of factor J_c which depends on pinning mechanism. The technical importance of HTSCs is found in power application for generators and motors etc., at 77 K i.e. boiling point of liquid nitrogen [1,2]. Inspite of much work involved in HTSCs material both theoretical and experimental still its origin remains an unsolved mystery.

Since the last decade, there have been several reports on effective pinning agents. Matsumoto and Mele [3] discusses widely on the variety of artificial pinning centers (APCs). Dimensionality of APCs varies as 1D — dislocations and columnar defects [4], 2D — APCs includes grain boundary, antiphases [5] etc., and 3D — APCs categories nanoparticles [6,7]. Among the secondary phases, silver is a well-known composite agent [8] and literature provides enough experimental evidences for its uniqueness. First, there exist no chemical interaction between Ag and YBCO. Second, Ag is not incorporated in lattice site of YBCO. Third, Ag resides in the intergranular boundaries of granular YBCO filling cracks and voids minimizing porosity of the system [9–11]. Other benefits of Ag are enhancing material property by providing extra oxygen to the growing film [12,13], increasing thermal and electrical conductivity [14].

Swift heavy ion irradiation (SHI) introduces 1D columnar defects. Tuning heavy energetic ions brings microstructural changes like ion implantations, columnar defects, point defects etc. Flux pinning property in superconductors is highly dependent on columnar defects which traps the moving vortex [15,16]. Effective trapping of vortices demands cross-sectional diameter of columnar defects of the order of ξ.

In this report we analyze the combined effect of Ag (secondary phase — 3D APCs) and SHI irradiation (1D — APCs) on YBCO film. The whole idea behind this work is to visualize the pinning impact and report the value of J_c. For its lattice parameter compatibility $LaAlO_3$ (LAO) substrate is used [17].

2. Experimental details

YBCO powder was prepared by solid state reaction route. Stoichiometric amount of high-purity powders of Y_2O_3, $BaCO_3$ and CuO precursors were grinded and calcined at 850 °C. Approximately 3 at. % Ag powders were mixed well with YBCO, pelletized and sintered at 920 °C which served as the target. YBCO/Ag films were deposited on (*l00*) oriented LAO single crystal substrates by the pulsed laser deposition (PLD). The growth conditions of thin film are summarized below in Table 1. The films of ~100 nm were irradiated with 200 MeV $107Ag^{+15}$ ions using the 15 MV tandem pelletron accelerator at IUAC, New Delhi. A total of 200 MeV of Ag ions has a projection range ~12 μm. Since projectile range is greater than the film thickness hence most of the Ag ions are expected to fully penetrate the superconducting

* Corresponding author. Tel.: +91 6612462724; fax: +91 6612462999.
E-mail address: dhrubananda_behera@yahoo.co.in (D. Behera).

0040-6090/$ – see front matter
http://dx.doi.org/10.1016/j.tsf.2013.03.089

Table 1
Growth condition for PLD film.

Laser	KrF excimer laser ($\lambda = 248$ nm)
Target	YBCO + Ag (3 at. %) pellet
substrate	(100)-oriented $LaAlO_3$ (LAO)
Target substrate distance	5 cm
Repetition frequency	10 Hz
Thickness	~100 nm
Laser energy	220 mJ
Substrate temperature	820 °C
Oxygen pressure	53.328 Pa

film. SHI creates uniformly distributed defect across the film thickness and avoids any effects of Ag doping. To prevent sample heating during irradiation, a low ion beam current (0.03 to 0.1 pnA) was maintained. Phase analysis was done using CuKα radiation by X-ray powder diffraction (XRD) (PW 3020 vertical goniometer and 3710 X' PertMPD control unit). The operating voltage and input current supplied are 30 kV and 20 mA respectively with $\theta - 2\theta$ geometry. Raman spectra were obtained using Ar ion laser with 514.5 nm wavelength and 50 mW power. Magnetization measurements were carried out using Quantum Design MPMS EverCool Dewar Model C-050. The 7 Tesla superconducting quantum interference device (SQUID) is made in U.S.A. The sensitivity of the device is better than 10^{-10} Am^2 providing 7 T longitudinal fields in the temperature range 2 K to 330 K. Magnetization hysteresis was conducted at 40 K. J_c was extracted and pinning force (F_p) was estimated.

3. Result and discussion

3.1. Phase analysis

Fig. 1 shows the XRD pattern of YBCO/Ag irradiated and non irradiated film of thickness ~100 nm. The pattern shows well defined peaks. Indexing of the pattern reveals that the films are orthorhombic in structure with space group *Pmmm*. Peaks in the graph shown have preferred orientation (00*l*) of YBCO. The substrate contribution is marked as LAO. No peaks of silver appear in the XRD pattern; it may be due to low concentration (3 at. %). SHI brings remarkable difference in the film. A total of 200 MeV Ag ions are known to bring about structural change i.e. columnar defects of the diameter of the order of ξ. After irradiation at fluence 5×10^{12} ions/cm^2 the changes noted are (i) peak intensity at (004) and (007) reduces to a great extent. (ii) The peaks shift to a lower angle value indicating an increase in *d* spacing caused by the strain of the incoming ions in the film. Biswal et al. [18] have shown that the complete amorphization occurs at fluence 2×10^{13} ions/cm^2 where peak (004), (007) is lost. SRIM gives calculative insight to understand the mechanism of ion track formation. A total of 200 MeV Ag ions having charged state +15 has an electronic energy loss (S_e) = 25.18 keV nm^{-1}, the threshold value (S_{th}) = 20 keV nm^{-1} and nuclear energy loss (S_n) = 0.071 keV nm^{-1} that travels a distance of ~12.66 μm in the film [19]. As $S_e > S_{th}$ amorphous ion tracks are formed along the ion path and penetrate deep into the substrate. Risk of Ag implantation in the film is eliminated as the range of ion is greater than the film thickness. These amorphized tracks are highly disoriented and have no contributions to XRD reflections. As the crystalline volume fraction decreases with exposure of ion irradiation, the intensity of (00*l*) peaks decreases. We also see a decrease in *a* and *b* parameters of the cell volume and an elongation along the *c* axis. This is attributed to radial stress generated by the SHI forming disordered amorphized latent tracks along the *c* axis. The parameters are tabulated in Table 2.

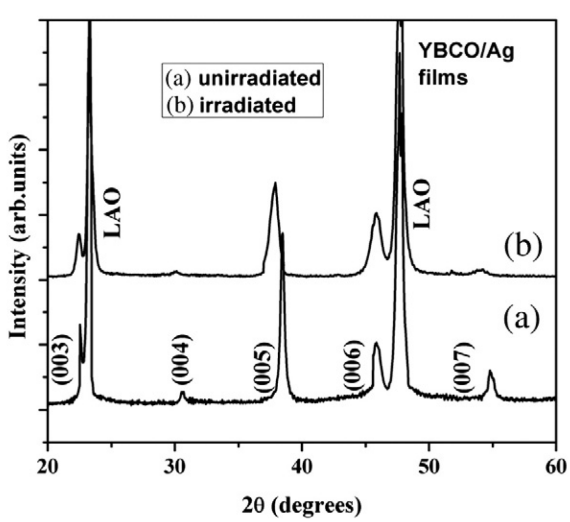

Fig. 1. XRD pattern of (a) YBCO/Ag thin film (b) YBCO/Ag thin film irradiated with 200 MeV Ag^{+15} ion with a dose of 5×10^{12} ions/cm^2.

3.2. Raman analysis

Fig. 2 shows the Raman spectrum of YBCO/Ag pristine and irradiated films. Five active vibrational modes in Raman spectra for pristine YBCO/Ag film are shown. A perovskite YBCO unit cell has five different oxygen sites which gets activated under the influx of photons: O (1) in CuO chains, O (2,3) in CuO_2 planes, O (4) in the apical chains and O (5) lie in between the oxygen chains and are empty in orthorhombic structure. The active vibrations of atoms along the *c* axis are identified at peak position ~502 cm^{-1}, ~440 cm^{-1}, ~340 cm^{-1} representing the stretching of apical oxygen or the bridging oxygen O (4) denoted as O (4) A_g, in the phase vibration of O (2)—O (3) oxygen atom in CuO_2 plane marked as O (2,3) A_g and out-of-phase *c* axis vibration of O (2)—O (3) oxygen atom in CuO_2 plane labeled as O (2,3) B_{1g} respectively [20]. The other two Raman active modes are vertical along the *c* axis given by Cu (2) atoms (~154 cm^{-1}) denoted as Cu (2) A_g and Ba atoms (~116 cm^{-1}) marked Ba A_g. Our data match well with different experimental and theoretical groups [21–23].

Act of 200 MeV Ag ions on the films resulted in significant changes in the spectra effecting different vibrational mode. Spectra (b) and (c) clearly show deactivation on apical oxygen at 500 cm^{-1}. The frequency of the apical oxygen line shifts to the lower frequency side; peak softening as well as broadening becomes significant upon irradiation. However the peak diminishes for a higher dose 5×10^{12} ions/cm^2. The frequency of the apical oxygen O (4) is associated with the oxygen stoichiometry of the YBCO films [24]. Huong et al. [25] have related frequency of the O (4) A_g Raman mode and oxygen content through the following empirical relationship.

$$\delta = 0.027\nu_A - 6.58 \quad (1)$$

where ν_A is the wave number of the O (4) A_g mode given in cm^{-1}. On the other hand, oxygen content is calculated from the *c* axis length using the following relationship [26,27]

$$\delta = (12.771 - c)/0.1557 \quad (2)$$

Table 2
Different parameters calculated using XRD pattern and Raman spectra. *c* is the lattice parameter along *Z* direction, *V* is volume of the unit cell, δ is oxygen content, ν_A is frequency of apical oxygen.

Sample	*c* (Å)	δ (from XRD)	ν_A (cm^{-1})	δ (from Raman)
YBCO/Ag	11.68(2)	0.19(2)	504	0.01(3)
5×10^{11} ions/cm^2	–	–	498	1.4(4)
5×10^{12} ions/cm^2	11.71(3)	0.37(3)	497	0.26(1)